We are IntechOpen, the world's leading publisher of Open Access books Built by scientists, for scientists

4,800
Open access books available

122,000
International authors and editors

135M
Downloads

Our authors are among the

154
Countries delivered to

TOP 1%
most cited scientists

12.2%
Contributors from top 500 universities

CLARIVATE ANALYTICS BOOK CITATION INDEX INDEXED

WEB OF SCIENCE™

Selection of our books indexed in the Book Citation Index in Web of Science™ Core Collection (BKCI)

Interested in publishing with us?
Contact book.department@intechopen.com

Numbers displayed above are based on latest data collected.
For more information visit www.intechopen.com

6

Feedback Linearization of Speed-Sensorless Induction Motor Control with Torque Compensation

Cristiane Cauduro Gastaldini[1], Rodrigo Zelir Azzolin[2], Rodrigo Padilha Vieira[3] and Hilton Abílio Gründling[4]
[1,2,3,4]*Federal University of Santa Maria*
[2]*Federal University of Rio Grande*
[3]*Federal University of Pampa*
Brazil

1. Introduction

This chapter addresses the problem of controlling a three-phase Induction Motor (IM) without mechanical sensor (i.e. speed, position or torque measurements). The elimination of the mechanical sensor is an important advent in the field of low and medium IM servomechanism; such as belt conveyors, cranes, electric vehicles, pumps, fans, etc. The absence of this sensor (speed, position or torque) reduces cost and size, and increases reliability of the overall system. Furthermore, these sensors are often difficult to install in certain applications and are susceptible to electromagnetic interference. In fact, sensorless servomechanism may substitute a measure value by an estimated one without deteriorating the drive dynamic performance especially under uncertain load torque.

Many approaches for IM sensorless servomechanism have been proposed in the literature is related to vector-controlled methodologies. One of the proposed nonlinear control methodologies is based on Feedback Linearization Control (FLC), as first introduced by (Marino et al., 1990). FLC provides rotor speed regulation, rotor flux amplitude decoupling and torque compensation. Although the strategy presented by (Marino et al., 1990) was not a sensorless control strategy, fundamental principles of FLC follow servomechanism design of sensorless control strategies, such as (Gastaldini & Grundling, 2009; Marino et al., 2004; Montanari et al., 2007; 2006).

The purpose of this chapter is to present the development of two FLC control strategies in the presence of torque disturbance or load variation, especially under low rotor speed conditions. Both control strategies are easily implemented in fixed point DSP, such as TMS320F2812 used on real time experiments and can be easily reproduced in the industry. Furthermore, an analysis comparing the implementation and the limitation of both strategies is presented. In order to implement the control law, these algorithms made use of only two-phase IM stator currents measurement. The values of rotor speed and load torque states used in the control algorithm are estimated using a Model Reference Adaptive System (MRAS) (Peng & Fukao, 1994) and a Kalman filter (Cardoso & Gründling, 2009), respectively.

This chapter is organized as follows: Section 2 presents the fifth-order IM mathematical model. Section 3 introduces the feedback linearization modelling of IM control. A simplified

FLC control strategy is described in Section 4. The proposed methods for speed and torque estimation, MRAS and Kalman filter algorithms, respectively, are developed in Sections 5 and 6. State variable filter is used to obtain derivative signals necessary for implementation of the control algorithm, and this is presented in section 7. Digital implementation in fixed point DSP TMS320F2812 and real time experimental results are given in Section 8. Finally, Section 9 presents the conclusions.

2. Induction motor mathematical model

A three-phase N pole pair induction motor is expressed in an equivalent two-phase model in an arbitrary rotating reference frame (q-d), according to (Krause, 1986) and (Leonhard, 1996) according to the fifth-order model, as

$$\frac{d}{dt}I_{qs} = -a_{12}I_{qs} - \omega_s I_{ds} + a_{13}a_{11}\lambda_{qr} - a_{13}N\omega\lambda_{dr} + a_{14}V_{qs} \tag{1}$$

$$\frac{d}{dt}I_{ds} = -a_{12}I_{ds} + \omega_s I_{qs} + a_{13}a_{11}\lambda_{dr} + a_{13}N\omega\lambda_{qr} + a_{14}V_{ds} \tag{2}$$

$$\frac{d}{dt}\lambda_{qr} = -a_{11}\lambda_{qr} - (\omega_s - N\omega)\,\lambda_{dr} + a_{11}L_m I_{qs} \tag{3}$$

$$\frac{d}{dt}\lambda_{dr} = -a_{11}\lambda_{dr} + (\omega_s - N\omega)\,\lambda_{qr} + a_{11}L_m I_{ds} \tag{4}$$

$$\frac{d}{dt}\omega = \mu \cdot \left(\lambda_{dr}I_{qs} - \lambda_{qr}I_{ds}\right) - \frac{B}{J}\omega - \frac{T_L}{J} \tag{5}$$

$$T_e = \mu \cdot J \cdot \left(\lambda_{dr}I_{qs} - \lambda_{qr}I_{ds}\right) \tag{6}$$

In equations (1)-(6): $\mathbf{I_s} = \left(I_{qs}, I_{ds}\right)$, $\boldsymbol{\lambda_r} = \left(\lambda_{qr}, \lambda_{dr}\right)$ and $\mathbf{V_s} = \left(V_{qs}, V_{ds}\right)$ denote stator current, rotor flux and stator voltage vectors, where subscripts d and q stand for vector components in (q-d) reference frame; ω is the rotor speed, the load torque T_L, electric torque T_e and ω_s is the stationary speed, θ_0 is the angular position of the (q-d) reference frame with respect to a fixed stator reference frame (α-β) , where physical variables are defined. Transformed variables related to three-phase (RST) system are given by

$$\mathbf{x_{\alpha\beta}} = \mathbf{K} \cdot \mathbf{x_{RST}} \tag{7}$$

Let

$$\mathbf{x_{qd}} = \mathbf{e}^{j\theta_0}\mathbf{x_{\alpha\beta}} \tag{8}$$

with $\mathbf{e}^{j\theta_0} = \begin{bmatrix} \cos\theta_0 & -\sin\theta_0 \\ \sin\theta_0 & \cos\theta_0 \end{bmatrix}$ and $\mathbf{K} = \sqrt{\frac{2}{3}}\begin{bmatrix} 1 & -\frac{1}{2} & -\frac{1}{2} \\ 0 & -\frac{\sqrt{3}}{2} & -\frac{\sqrt{3}}{2} \end{bmatrix}$.

$\mathbf{x_{qd}}$ and $\mathbf{x_{\alpha\beta}}$ stand for two-dimensional voltage flux and stator current vector, respectively on (q-d) and (α-β)reference frame.

The relations between mechanical and electrical parameters in the above equations are $a_0 \triangleq L_s L_r - L_m^2$, $a_{11} \triangleq \frac{R_r}{L_r}$, $a_{12} \triangleq \left(\frac{L_s L_r}{a_0}\frac{R_s}{L_s} + \frac{L_m^2}{a_0}a_{11}\right)$, $a_{13} \triangleq \frac{L_m}{a_0}$, $a_{14} \triangleq \frac{L_r}{a_0}$ and $\mu \triangleq \frac{NL_m}{JL_r}$;

where R_s, R_r, L_s and L_r are the stator/rotor resistances and inductances, L_m is the magnetizing inductance, J is the rotor inertia, B is the viscous coefficient and N is the number of pole pairs. In the control design, the viscous coefficient of (5) is considered to be approximately zero, i.e. $B \approx 0$.

3. Feedback Linearization Control

The feedback Linearization Control (FLC) general specifications are two outputs - rotor speed and rotor flux modulus, as

$$\mathbf{y_1} = \begin{bmatrix} \omega & \sqrt{\lambda_{qr}^2 + \lambda_{dr}^2} \end{bmatrix}^T \triangleq \begin{bmatrix} \omega & |\boldsymbol{\lambda}_\mathbf{r}| \end{bmatrix}^T \tag{9}$$

which is controlled by two-dimensional stator voltage vector $\mathbf{V_s}$, on the basis of measured variables vector $\mathbf{y}_2 = \mathbf{I_s}$. The development concept of this control strategy is completely described in (Marino et al., 1990) and it will be omitted here. Following the concept of indirect field orientation developed by Blaschke, (Krause, 1986) and (Leonhard, 1996), the purpose of FLC control is to align rotor flux vector with the d-axis reference frame, i.e.

$$\lambda_{dr} = |\boldsymbol{\lambda}_\mathbf{r}| \qquad \lambda_{qr} = 0 \tag{10}$$

The condition expressed in (10) guarantees the exact decoupling of flux dynamics of (1)-(4) from the speed dynamics. Once rotor flux is not directly measured, only asymptotic field orientation is possible, according to (Marino et al., 1990) and (Peresada & Tonielli, 2000), then

$$\lim_{t\to\infty} \lambda_{dr} = |\boldsymbol{\lambda}_\mathbf{r}| \qquad \lim_{t\to\infty} \lambda_{qr} = 0 \tag{11}$$

It is defined $\mathbf{y_1^*} = \begin{bmatrix} \omega_{ref} & \lambda_r^* \end{bmatrix}^T$, where ω_{ref} and λ_r^* are reference trajectories of rotor speed and rotor flux. The speed tracking, flux regulation control problem under speed sensorless conditions is formulated considering IM model (1)-(5) under the following conditions:
(a) Stator currents are measurable;
(b) Motor parameters are known and considered constant;
(c) Load torque is estimated and it is applied after motor flux excitation;
(d) Initial conditions of IM state variables are known;
(e) λ_r^* is the flux constant reference value and estimated speed $\widehat{\omega}$ and reference speed ω_{ref} are the smooth reference bounded speed signals.
FLC equations are developed considering the fifth-order IM model under the assumption that estimated speed tracks real speed, and therefore it is acceptable to replace measured speed with estimated speed (i.e. $\widehat{\omega}_k \approx \omega$). In addition, the torque value is estimated using a Kalman filter. Fig. 1 presents the block diagram of FLC Control.

3.1 Flux controller

From the decoupling properties of field oriented transformation (10), the control objective of the flux controller is to generate a flux vector aligned with the d-axis to guarantee induction motor magnetization.
Then, substituting (10) in (4)

$$i_{ds}^* = \left(a_{11}\lambda_r^* + \frac{d}{dt}|\boldsymbol{\lambda}_\mathbf{r}| \right) \frac{1}{a_{11}L_m} \tag{12}$$

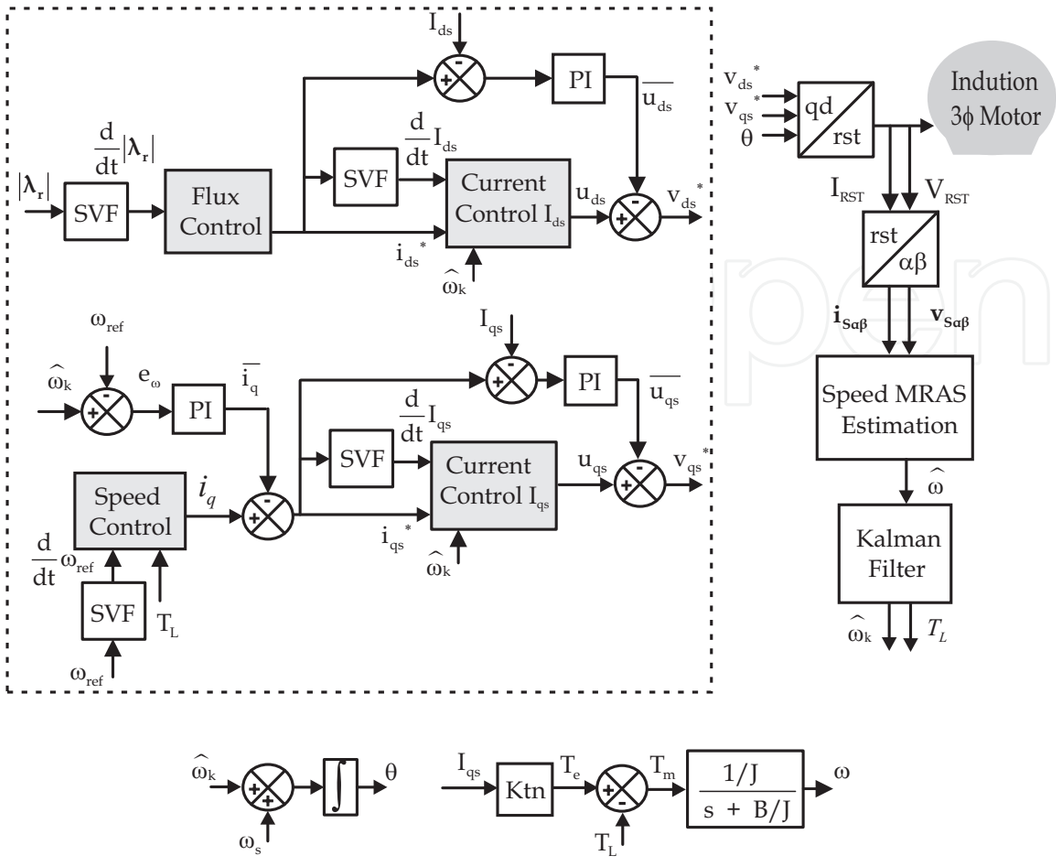

Fig. 1. Feedback Linearization Control proposed

The rotor flux $|\boldsymbol{\lambda}_\mathbf{r}|$ is estimated by a model derived from the induction motor mathematical model, (3) and (4), that makes use of measured stator currents $\left(I_{qs}, I_{ds}\right)$ and estimated speed $\widehat{\omega}$ variables.

$$\frac{d}{dt}\boldsymbol{\lambda}_\mathbf{r} = -a_{11}\boldsymbol{\lambda}_\mathbf{r} - j\left(\omega_s - N\omega\right)\boldsymbol{\lambda}_\mathbf{r} + a_{11}L_m\mathbf{I_s} \tag{13}$$

where the stationary speed is $\omega_s = N\widehat{\omega} + \frac{a_{11}L_m}{\lambda^*}i_{qs}^*$. The digital implementation of the flux controller is made using Euler discretization and the derivative rotor flux signal is obtained by a state variable filter (SVF).

3.2 Speed controller

The speed control algorithm uses the same strategy adopted for the flux subsystem and it is computed from (5), as

$$i_q = \frac{1}{\mu\lambda_r^*}\left(\frac{\widehat{T}_L}{J} + \frac{d}{dt}\omega_{ref}\right) \tag{14}$$

To compensate for speed error between estimated speed and reference speed, (i.e. $e_\omega = \widehat{\omega} - \omega_{ref}$), a proportional integral compensation is proposed, as follows

$$\overline{i_q} = \left(k_{p\_iq} + \frac{k_{i\_iq}}{s} \right) e_\omega \tag{15}$$

These gains values (k_{p_iq}, k_{i_iq}) are determined considering an induction motor mechanical model. The reference quadrature component stator speed current is derived from (14)-(15), as

$$i_{qs}^* = i_q - \overline{i_q} \tag{16}$$

In DSP implementation, the speed controller is discretized using the Euler method and the rotor speed derivative (14) is computed by a SVF.

3.3 Currents controller

From (1) and (2), the currents controller is obtained, as

$$u_{qs} = \frac{1}{a_{14}} \left(a_{12} i_{qs}^* + \omega_s i_{ds}^* + a_{13} \lambda_r^* N \left(\omega_{ref} + e_\omega \right) + \frac{d}{dt} I_{qs} \right) \tag{17}$$

and

$$u_{ds} = \frac{1}{a_{14}} \left(a_{12} i_{ds}^* + \omega_s i_{qs}^* + a_{11} a_{13} \lambda_r + \frac{d}{dt} I_{ds} \right) \tag{18}$$

where proportional integral gains of the current error

$$\overline{u}_{qs} = \left(k_{pv} + \frac{k_{iv}}{s} \right) \widetilde{i}_{qs} \tag{19}$$

and

$$\overline{u}_{ds} = \left(k_{pv} + \frac{k_{iv}}{s} \right) \widetilde{i}_{ds} \tag{20}$$

in which $\widetilde{i}_{qs} = I_{qs} - i_{qs}^*$ and $\widetilde{i}_{ds} = I_{ds} - i_{ds}^*$.
These gains (k_{pv}, k_{iv}) are determined considering a simplified induction motor electrical model, which is obtained by load and locked rotor test. Hence, current controllers are expressed as

$$v_{qs}^* = u_{qs} - \overline{u}_{qs} \tag{21}$$

$$v_{ds}^* = u_{ds} - \overline{u}_{ds} \tag{22}$$

In DSP, currents controller are digitally implemented using discretized equation (17)-(22) based on the Euler method, and the stator current derivative is obtained by SVF using stator currents measures.

4. Simplified feedback linearization control

In order to reduce the number of computation requirements, a simplified feedback linearization control scheme is proposed. In this control scheme, one part of the current controller (6)-(7) is suppressed and only a proportional integral controller is used. This modification minimizes the influence of parameters variation in the control system.
Fig. 2 presents the block diagram of the Simplified FLC proposed.
The currents controller of simplified FLC are defined as

$$v_{qs}^{*} = \left(k_{pv} + \frac{k_{iv}}{s}\right)\widetilde{i}_{qs} \tag{23}$$

$$v_{ds}^{*} = \left(k_{pv} + \frac{k_{iv}}{s}\right)\widetilde{i}_{ds} \tag{24}$$

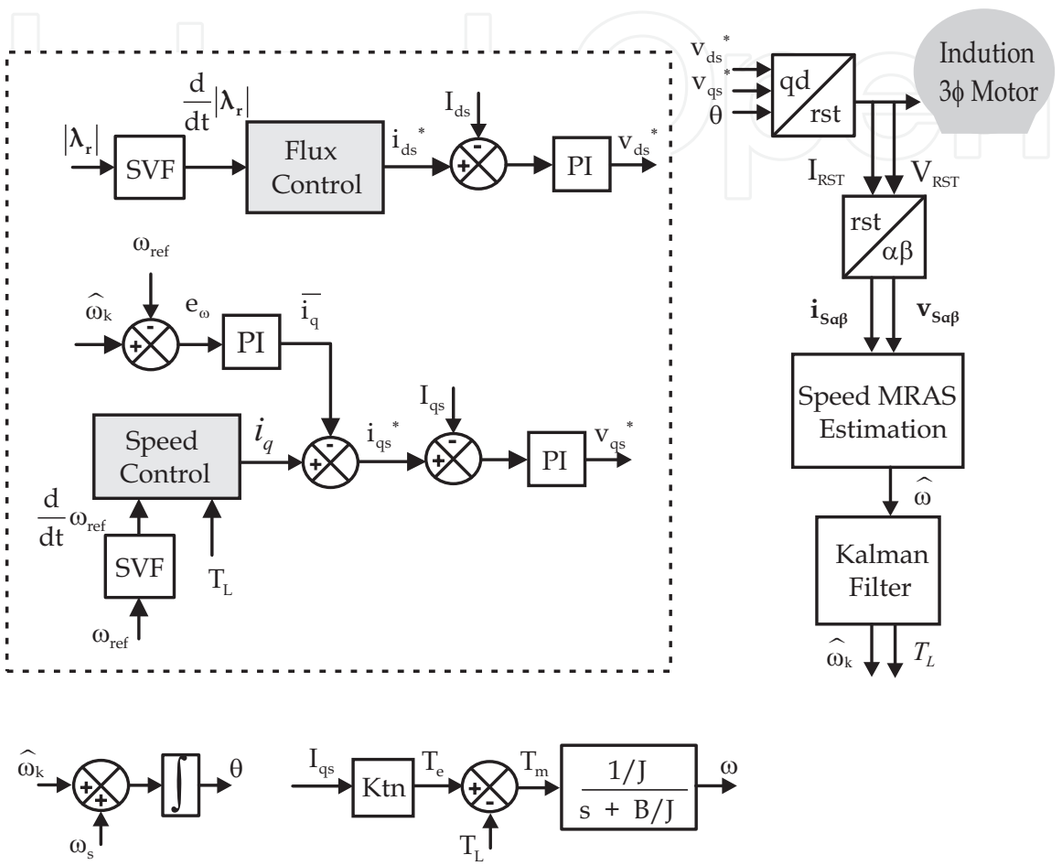

Fig. 2. Proposed Simplified Feedback Linearization Control

Flux and Speed Controller are computed exactly as in the previous scheme, as (12) and (14)-(16).

5. Speed estimation - MRAS algorithm

A squirrel-cage three-phase induction motor model expressed in a stationary frame can be modelled using complex stator and rotor voltage as in (Peng & Fukao, 1994)

$$\mathbf{v_s} = R_s\mathbf{i_s} + L_s\frac{d}{dt}\mathbf{i_s} + L_m\frac{d}{dt}\mathbf{i_r} \tag{25}$$

for squirrel-cage IM $\mathbf{v_r} = 0$

$$0 = R_r\mathbf{i_r} - jN\omega L_r\mathbf{i_r} - jN\omega L_m\mathbf{i_s} + L_r\frac{d}{dt}\mathbf{i_r} + L_m\frac{d}{dt}\mathbf{i_s} \tag{26}$$

The voltage and the current space vectors are given as $\overline{\mathbf{x}} = x_\alpha + jx_\beta$, $\overline{\mathbf{x}} \in \{\mathbf{v_s}, \mathbf{i_s}, \mathbf{i_r}\}$, relative to the transformed variables present in (7). The induction motor magnetizing current is expressed by

$$\mathbf{i_m} = \frac{L_r}{L_m}\mathbf{i_r} + \mathbf{i_s} \tag{27}$$

Two independent observers are derived to estimate the components of the counter-electromotive vectors.

$$\widehat{\mathbf{e}}_\mathbf{m} = \frac{L_m^2}{L_r}\mathbf{i_m} = \frac{L_m^2}{L_r}\left(\omega \mathbf{i_m} - \frac{1}{T_r}\mathbf{i_m} + \frac{1}{T_r}\mathbf{i_s}\right) \tag{28}$$

$$\mathbf{e_m} = \mathbf{v_s} - R_s\mathbf{i_s} - \sigma L_s \frac{d}{dt}\mathbf{i_s} \tag{29}$$

where $\sigma = 1 - \dfrac{L_m}{L_s L_r}$. The instantaneous reactive power maintains the magnetizing current, and its value is defined by cross product of the counter-electromotive and stator current vector

$$\mathbf{q_m} = \mathbf{i_s} \otimes \mathbf{e_m} \tag{30}$$

Substituting (28) and (29) for $\mathbf{e_m}$ in (30) and noting that $\mathbf{i_s} \otimes \mathbf{i_s} = 0$, which gives

$$\mathbf{q_m} = \mathbf{i_s} \otimes \left(\mathbf{v_s} - \sigma L_s \frac{d}{dt}\mathbf{i_s}\right) \tag{31}$$

and

$$\widehat{\mathbf{q}}_\mathbf{m} = \frac{L_m^2}{L_r}\left(\left(\mathbf{i_m} \odot \mathbf{i_s}\right)\omega + \frac{1}{T_r}\left(\mathbf{i_m} \otimes \mathbf{i_s}\right)\right) \tag{32}$$

Then, $\mathbf{q_m}$ is the reference model of reactive power and $\widehat{\mathbf{q}}_\mathbf{m}$ is the adjustable model. The estimated speed is produced by the proportional integral adaptation mechanism error of both models, and an MRAS system can be drawn as in Fig.3

This algorithm is customary for speed estimation and simple to implement in fixed point DSP, such as in (Gastaldini & Grundling, 2009; Orlowska-Kowalska & Dybkowski, 2010; Vieira et al., 2009).

The SVF blocks are state variable filters and are explained in greater detail in Section 7. These filters compute derivative signals and are applied in voltage signals to avoid addition noise and phase delay among the vectors as was proposed by (Martins et al., 2006).

6. Load torque estimation - Kalman filter

The reduced mechanical IM system can be represented by the following equations

$$\frac{d}{dt}\begin{bmatrix} \omega \\ T_L \end{bmatrix} = \begin{bmatrix} -\dfrac{B_n}{J} & -\dfrac{1}{J} \\ 0 & 0 \end{bmatrix}\begin{bmatrix} \omega \\ T_L \end{bmatrix} + \begin{bmatrix} \dfrac{1}{J} \\ 0 \end{bmatrix} T_e \tag{33}$$

$$y = \begin{bmatrix} 1 & 0 \end{bmatrix}\begin{bmatrix} \omega \\ T_L \end{bmatrix} \tag{34}$$

The Kalman Filter could be used to provide the value of torque load or disturbances - T_L. Since (15)-(16) is nonlinear, the Kalman filter linearizes the model at the actual operating

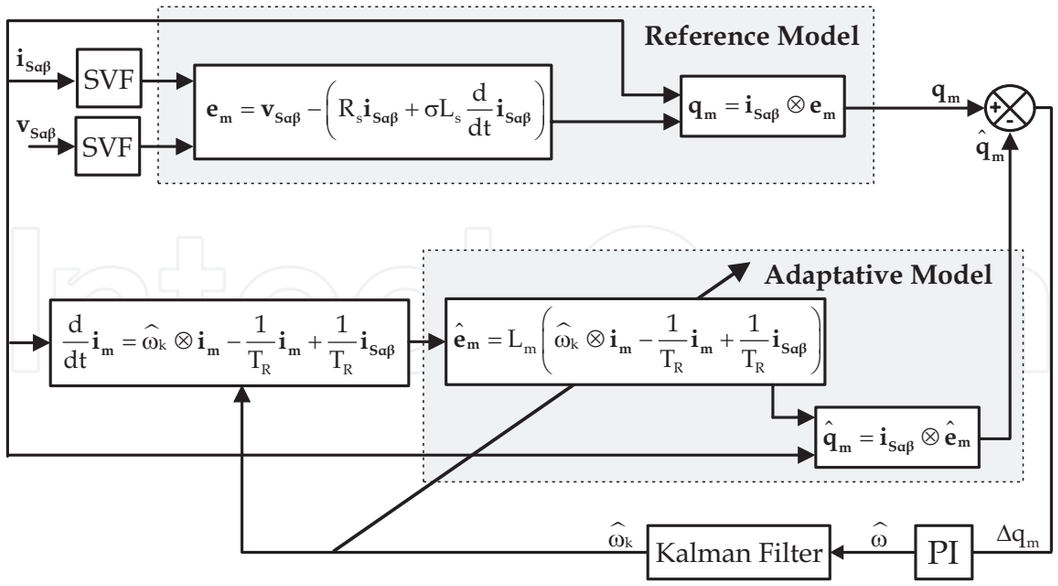

Fig. 3. Reactive Power MRAS Speed Estimation

point (Aström & Wittenmark, 1997). In addition, this filter takes into account the signal noise, which could be generated as pulse width modulation drivers. Assuming the definitions $\mathbf{x}_k = \begin{bmatrix} \widehat{\omega}_k & \widehat{T}_L \end{bmatrix}^T$, $\mathbf{A_m} = \begin{bmatrix} -\frac{B_n}{J} & -\frac{1}{J} \\ 0 & 0 \end{bmatrix}$, $\mathbf{B_m} = \begin{bmatrix} \frac{1}{J} \\ 0 \end{bmatrix}$, $\mathbf{C_m} = \begin{bmatrix} 1 & 0 \end{bmatrix}$ and $y_k = \widehat{\omega}$. Then, the recursive equation for the discrete time Kalman Filter (De Campos et al., 2000) is described by

$$\mathbf{K}(k) = \mathbf{P}(k)\mathbf{C}_\mathbf{m}^T \left(\mathbf{C_m}\mathbf{P}(k)\mathbf{C}_\mathbf{m}^T + \mathbf{R}\right)^{-1} \tag{35}$$

where $\mathbf{K}(k)$ is the Kalman gain. The covariance matrix $\mathbf{P}(k)$ is given by

$$\mathbf{P}(k+1) = (\mathbf{I} - \mathbf{A_m}t_s)\left(\mathbf{P}(k) - \mathbf{K}(k)\mathbf{C_m}\mathbf{P}(k)\right)(\mathbf{I} - \mathbf{A_m}t_s)^T + (\mathbf{B_m}t_s)\,\mathbf{Q}\,(\mathbf{B_m}t_s)^T \tag{36}$$

Therefore, the estimated torque $\widehat{T}_L$ is one observed state of the Kalman filter

$$\widehat{\mathbf{x}}_\mathbf{k}(k+1) = (\mathbf{I} - \mathbf{A_m}t_s)\,\widehat{\mathbf{x}}_\mathbf{k}(k) + \mathbf{B_m}t_s u(k) + (\mathbf{I} - \mathbf{A_m}t_s)\,\mathbf{K}(k)\left(\widehat{\omega} - \mathbf{C_m}\widehat{\mathbf{x}}_\mathbf{k}(k)\right) \tag{37}$$

giving $\widehat{\omega} \approx \widehat{\omega}_k$ and $\widehat{\mathbf{x}}_\mathbf{k}(k) = \begin{bmatrix} \widehat{\omega}_k & T_L \end{bmatrix}^T$.
The matrices $\mathbf{R}$ and $\mathbf{Q}$ are defined according to noise elements of predicted state variables, taking into account the measurement noise covariance $\mathbf{R}$ and the plant noise covariance $\mathbf{Q}$.

7. State variable filter

The state variable filter (SVF) is used to mathematically evaluate differentiation signals. This filter is necessary in the implementation of FLC and MRAS algorithms. The transfer function of SVF is of second order as it is necessary to obtain the first order derivative.

$$G_{svf} = \frac{\omega_{svf}}{\left(s + \omega_{svf}\right)^2} \tag{38}$$

where ω_{svf} is the filter bandwidth defined at around 5 to 10 times the input frequency signal u_{svf}.
The discretized transfer function, using the Euler method, can be performed in state-space as

$$\mathbf{x_{svf}}(k+1) = \mathbf{A_{svf}}\mathbf{x_{svf}}(k) + \mathbf{B_{svf}}u_{svf}(k) \tag{39}$$

where $\mathbf{A_{svf}} = \begin{bmatrix} 1 & 1 \\ -\omega_{svf}^2 & 1-2\omega_{svf} \end{bmatrix}$, $\mathbf{B_{svf}} = \begin{bmatrix} 0 \\ \omega_{\text{svf}}^2 \end{bmatrix}$ and $\mathbf{x_{svf}} = \begin{bmatrix} x_1 \\ x_2 \end{bmatrix}$.
The state variables x_1 and x_2 represent the input filtered signal and input derivative signal.

8. Experimental results

Sensorless control schemes were implemented in DSP based platform using TMS 320F2812. Experimental results were carried out on a motor with specifications: 1.5cv, 380V, 2.56A, 60 Hz, $R_s = 3.24\Omega$, $R_r = 4.96\Omega$, $L_r = 404.8mH$, $L_s = 402.4mH$, $L_m = 388.5mH$, $N = 2$ and nominal speed of 188 rad/s.
The experimental analyses are carried out with the following operational sequence:
1) The motor is excited (during 10 s to 12 s) using a smooth flux reference trajectory.
2) Starting from zero initial value, the rotor speed reference grows linearly until it reaches the reference value. Thus, the reference rotor speed value is kept constant.
3) During stand-state, a step constant load torque is applied.
In order to generate load variation for torque disturbance analyses, the DC motor is connected to an induction motor driving-shaft. Then, the load shaft varies in accordance with DC motor field voltage and inserting a resistance on its armature. Fig. 4 and Fig. 5 depict performance of both control schemes: FLC control and simplified FLC control with rotor speed reference of 18 rad/s. In these figures measure speed, estimated speed, stator (q-d) currents and estimated torque are illustrated.
Fig.6 and Fig. 7 present experimental results with 36 rad/s rotor speed reference.
Fig. 8 and Fig. 9 show FLC control and Simplified FLC with 45 rad/s rotor speed reference.
The above figures present experimental results for low rotor speed range of FLC control and Simplified FLC control applying load torque. In accordance with the figures above, both control schemes present similar performances in steady state. It is verified that both schemes respond to compensated torque variations. With respect to Simplified FLC, it is necessary to carrefully select fixed gains in order to guarantee the alignment of the rotor flux on the d axis.

9. Conclusion

Two different sensorless IM control schemes were proposed and developed based on nonlinear control - FLC Control and Simplified FLC Control. These control schemes are composed of a flux-speed controller, which is derived from a fifth-order IM model. In the implementation of feedback linearization control (FLC), the control algorithm presents a large number of computational requirements. In the simplified FLC scheme, a substitution of FLC currents controllers by two PI controllers is proposed to generate the stator drive voltage. In order to provide the rotor speed for both control schemes, a MRAS algorithm based on reactive power is applied.
To correctly evaluate whether this Simplified FLC does not affect control performance, a comparative experimental analysis of a FLC control and a simplified FLC control is presented. Experimental results in DSP TMS 320F2812 platform show the performance of both systems

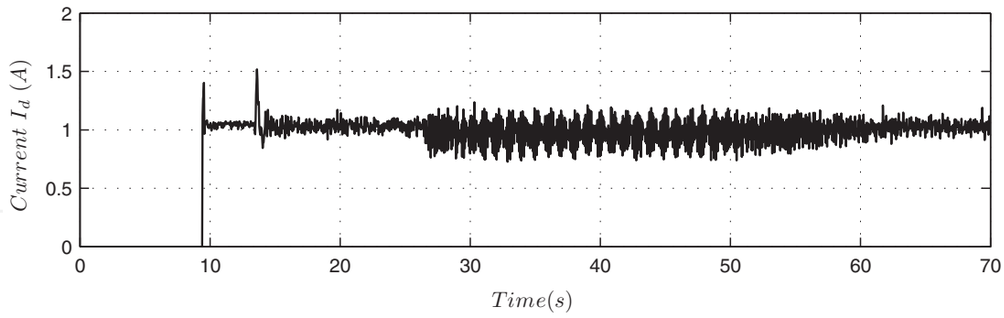

(a) IM Stator Current I_{ds}

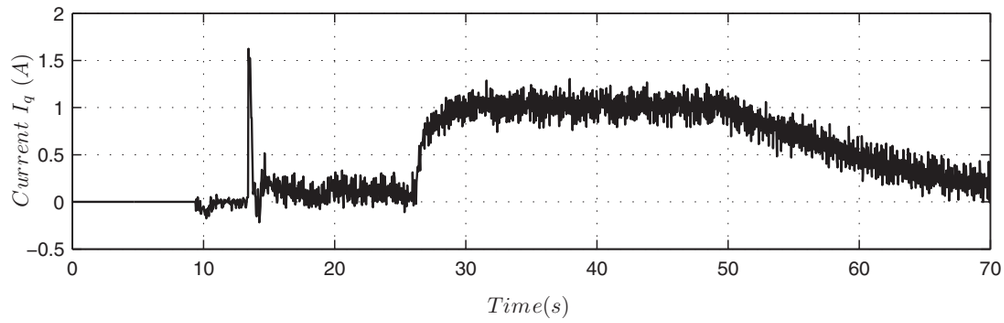

(b) IM Stator Current I_{qs}

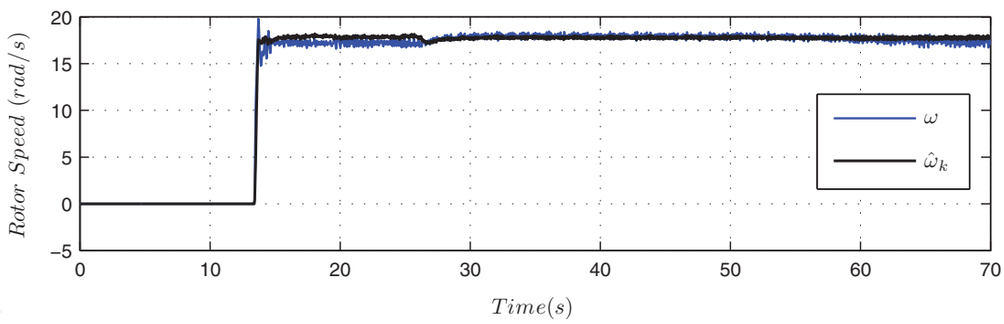

(c) Rotor Speed - Estimated and Encoder Measurement

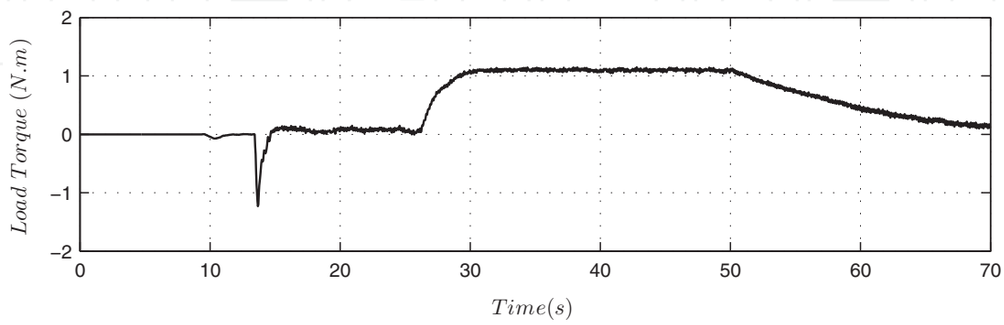

(d) Estimated Load Torque

Fig. 4. FLC control with 18 rad/s rotor speed reference

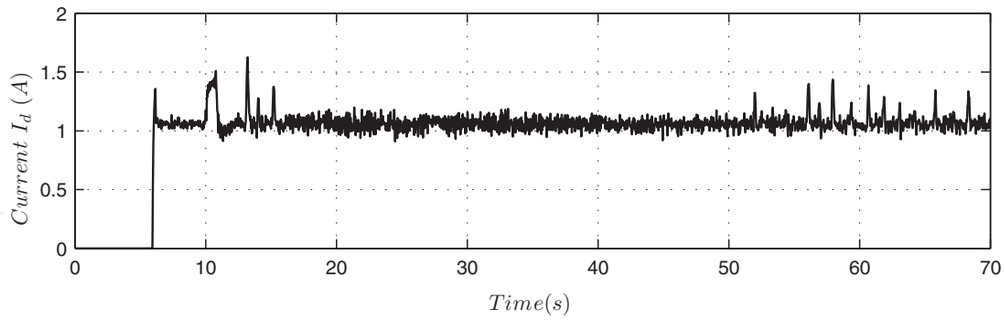

(a) IM Stator Current I_{ds}

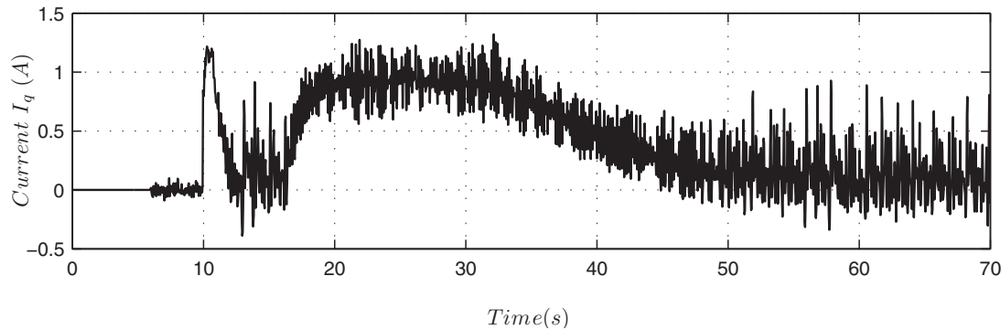

(b) IM Stator Current I_{qs}

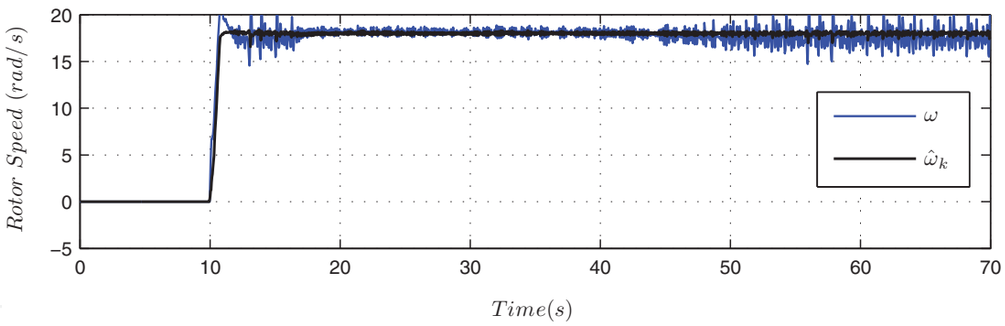

(c) Rotor Speed - Estimated and Encoder Measurement

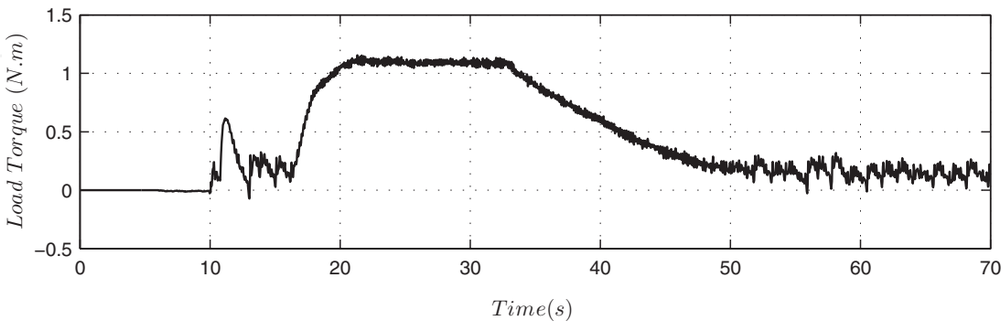

(d) Estimated Load Torque

Fig. 5. Simplified FLC control with 18 rad/s rotor speed reference

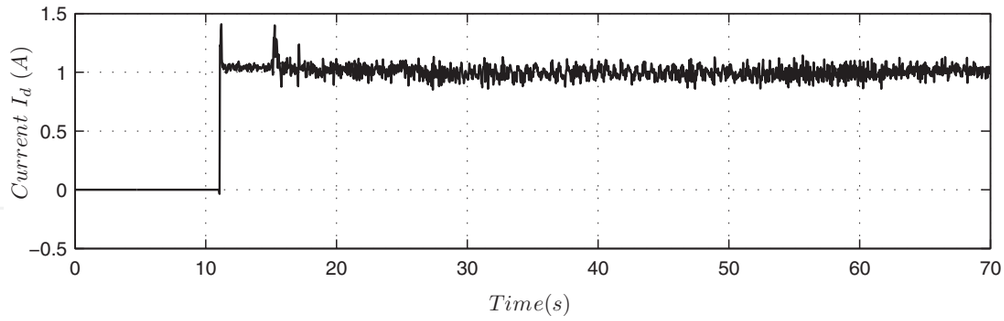

(a) IM Stator Current I_{ds}

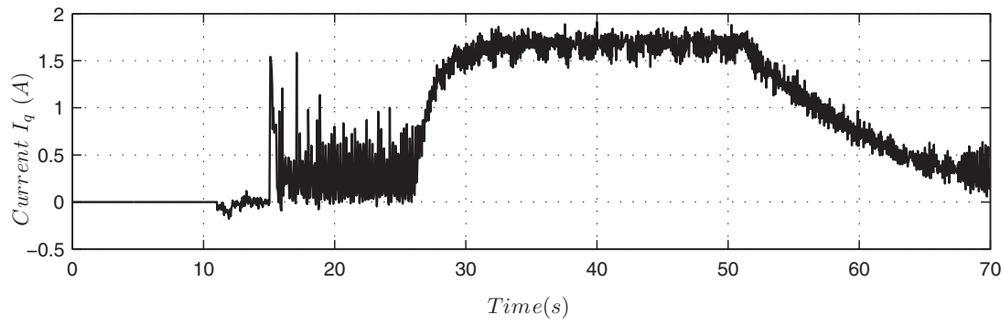

(b) IM Stator Current I_{qs}

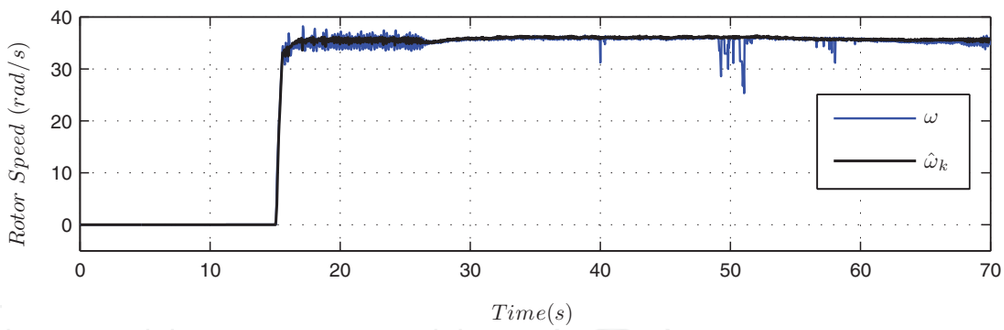

(c) Rotor Speed - Estimated and Encoder Measurement

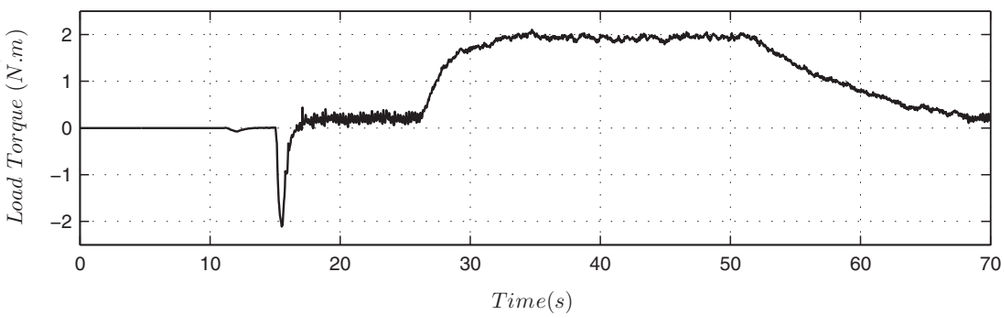

(d) Estimated Load Torque

Fig. 6. FLC control with 36 rad/s rotor speed reference

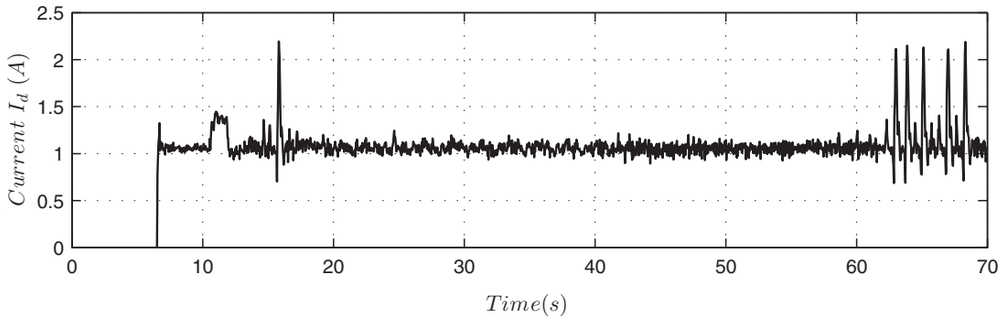

(a) IM Stator Current I_{ds}

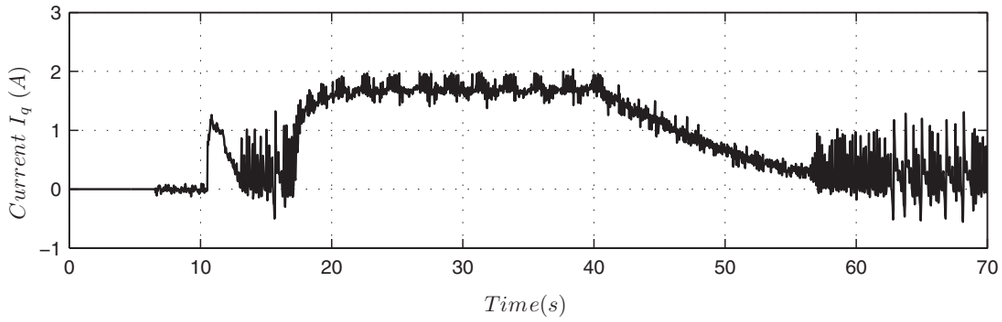

(b) IM Stator Current I_{qs}

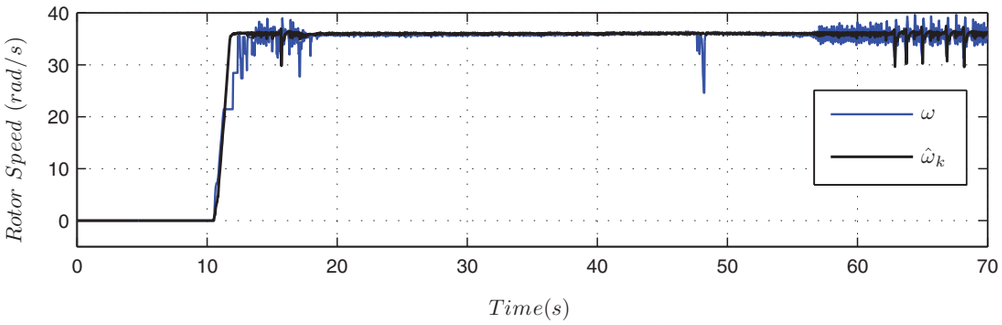

(c) Rotor Speed - Estimated and Encoder Measurement

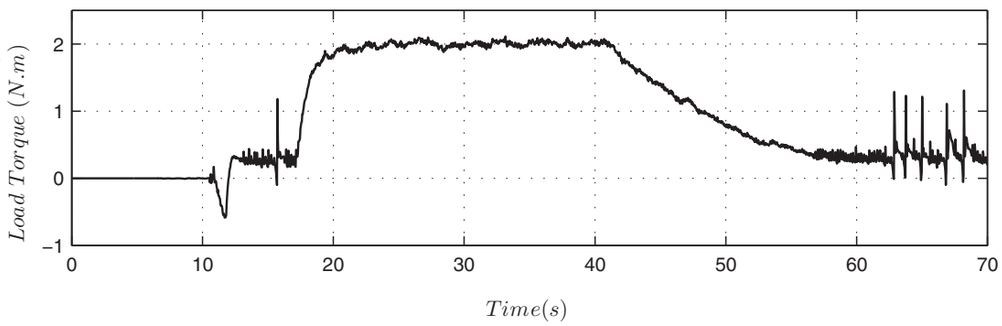

(d) Estimated Load Torque

Fig. 7. Simplified FLC control with 36 rad/s rotor speed reference

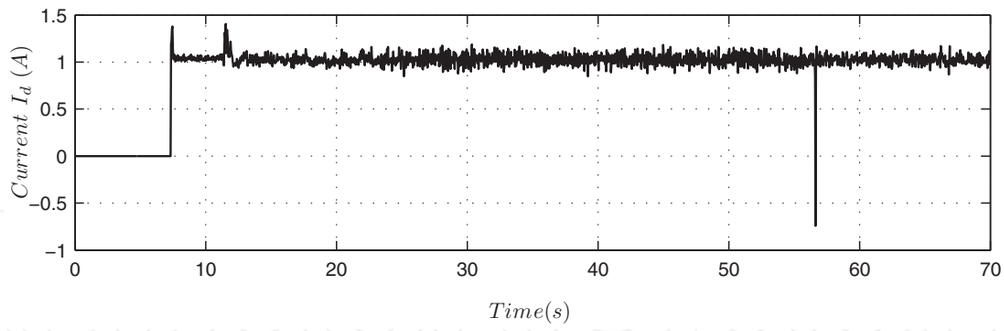

(a) IM Stator Current I_{ds}

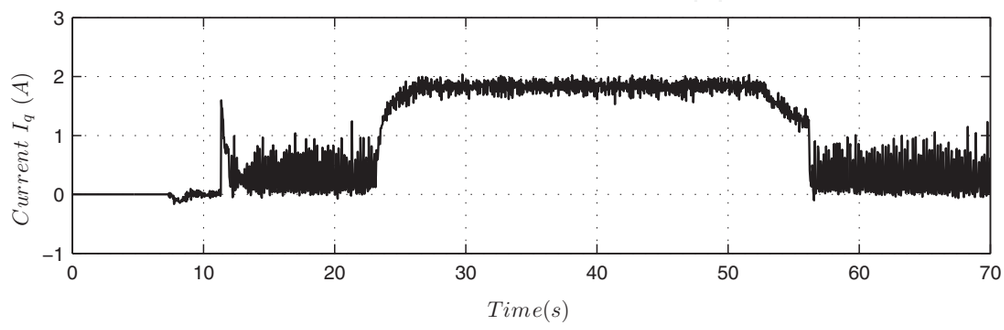

(b) IM Stator Current I_{qs}

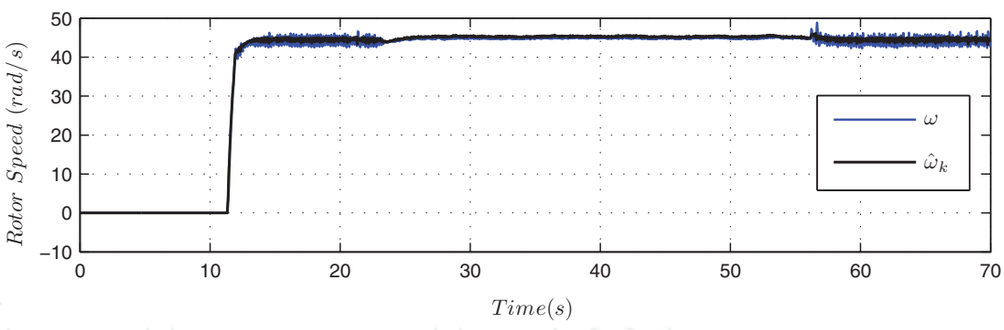

(c) Rotor Speed - Estimated and Encoder Measurement

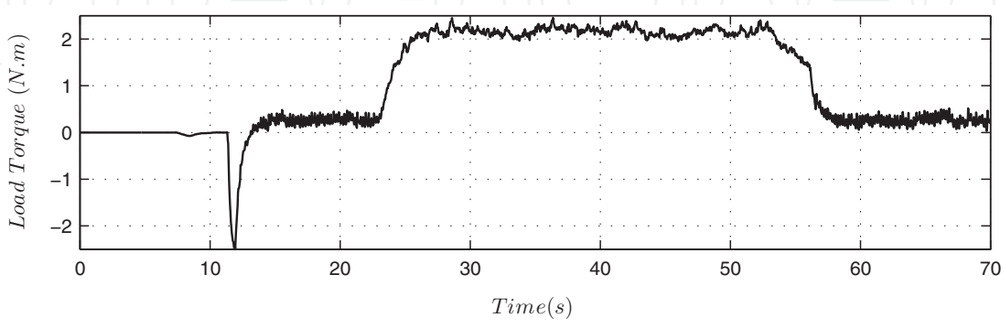

(d) Estimated Load Torque

Fig. 8. FLC control with 45 rad/s rotor speed reference

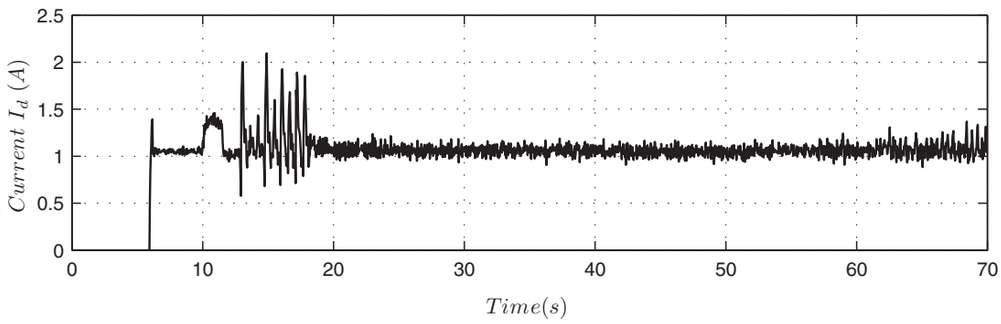

(a) IM Stator Current I_{ds}

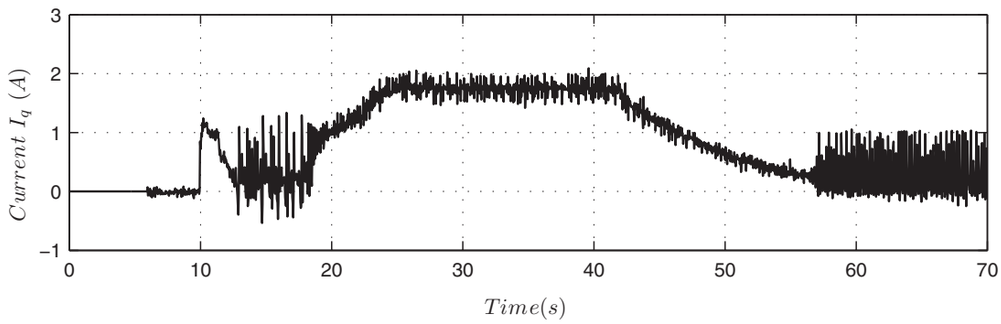

(b) IM Stator Current I_{qs}

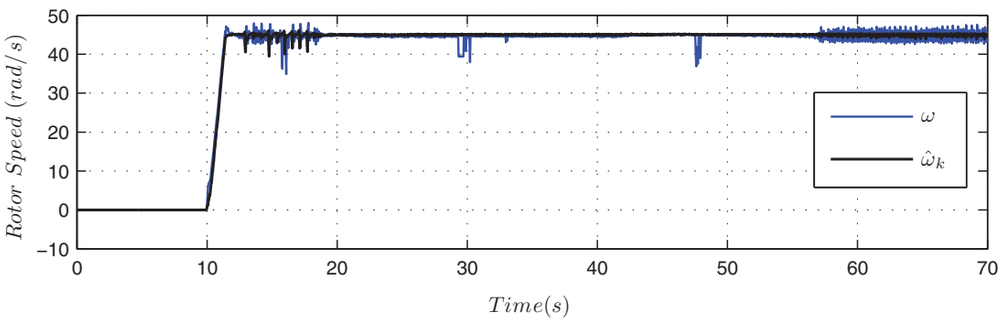

(c) Rotor Speed - Estimated and Encoder Measurement

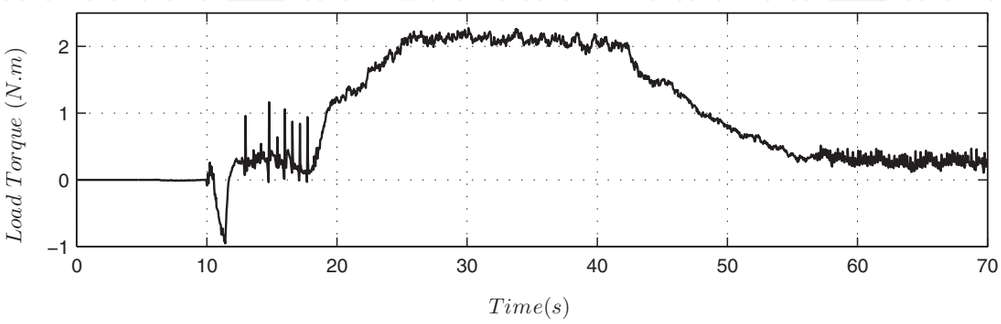

(d) Estimated Load Torque

Fig. 9. Simplified FLC control with 45 rad/s rotor speed reference

in the 18rad/s, 36 rad/s and 45 rad/s rotor speed range. Both control schemes present similar performance in steady-state. Hence, the proposed modification of the FLC control allows a simplification of the control algorithm without deterioration in control performance. However, it may necessary to carefully evaluate the gain selection in the simplified FLC control, to guarantee rotor flux alignment on the d axis, as well as, to guarantee speed-flux decoupling. Both control schemes indicate sensitivity with model parameter variation, and one way to overcome this would be the is development of an adaptive FLC control laws on FLC control.

10. References

Aström, K. & Wittenmark, B. (1997). *Computer-Controlled Systems: Theory and Design*, Prentice-Hall.

Cardoso, R. & Gründling, H. A. (2009). Grid synchronization and voltage analysis based on the kalman filter, *in* V. M. Moreno & A. Pigazo (eds), *Kalman Filter Recent Advances and Applications*, InTech, Croatia, pp. 439–460.

De Campos, M., Caratti, E. & Grundling, H. (2000). Design of a position servo with induction motor using self-tuning regulator and kalman filter, *Conference Record of the 2000 IEEE Industry Applications Conference, 2000*.

Gastaldini, C. & Grundling, H. (2009). Speed-sensorless induction motor control with torque compensation, *13th European Conference on Power Electronics and Applications, EPE '09*, pp. 1 –8.

Krause, P. C. (1986). *Analysis of electric machinery*, McGraw-Hill.

Leonhard, W. (1996). *Control of Electrical Drives*, Springer-Verlag.

Marino, R., Peresada, S. & Valigi, P. (1990). Adaptive partial feedback linearization of induction motors, *Proceedings of the 29th IEEE Conference on Decision and Control, 1990*, pp. 3313 –3318 vol.6.

Marino, R., Tomei, P. & Verrelli, C. M. (2004). A global tracking control for speed-sensorless induction motors, *Automatica* 40(6): 1071 – 1077.

Martins, O., Camara, H. & Grundling, H. (2006). Comparison between mrls and mras applied to a speed sensorless induction motor drive, *37th IEEE Power Electronics Specialists Conference, PESC '06.*, pp. 1 –6.

Montanari, M., Peresada, S., Rossi, C. & Tilli, A. (2007). Speed sensorless control of induction motors based on a reduced-order adaptive observer, *IEEE Transactions on Control Systems Technology* 15(6): 1049 –1064.

Montanari, M., Peresada, S. & Tilli, A. (2006). A speed-sensorless indirect field-oriented control for induction motors based on high gain speed estimation, *Automatica* 42(10): 1637 – 1650.

Orlowska-Kowalska, T. & Dybkowski, M. (2010). Stator-current-based mras estimator for a wide range speed-sensorless induction-motor drive, *IEEE Transactions on Industrial Electronics* 57(4): 1296 –1308.

Peng, F.-Z. & Fukao, T. (1994). Robust speed identification for speed-sensorless vector control of induction motors, *IEEE Transactions on Industry Applications* 30(5): 1234 –1240.

Peresada, S. & Tonielli, A. (2000). High-performance robust speed-flux tracking controller for induction motor, *International Journal of Adaptive Control and Signal Processing, 2000*.

Vieira, R., Azzolin, R. & Grundling, H. (2009). A sensorless single-phase induction motor drive with a mrac controller, *35th Annual Conference of IEEE Industrial Electronics,IECON '09.*, pp. 1003 –1008.

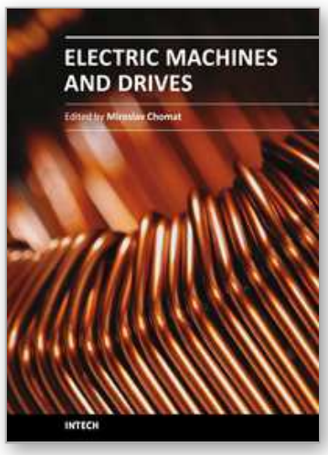

Electric Machines and Drives

Edited by Dr. Miroslav Chomat

ISBN 978-953-307-548-8
Hard cover, 262 pages
Publisher InTech
Published online 28, February, 2011
Published in print edition February, 2011

The subject of this book is an important and diverse field of electric machines and drives. The twelve chapters of the book written by renowned authors, both academics and practitioners, cover a large part of the field of electric machines and drives. Various types of electric machines, including three-phase and single-phase induction machines or doubly fed machines, are addressed. Most of the chapters focus on modern control methods of induction-machine drives, such as vector and direct torque control. Among others, the book addresses sensorless control techniques, modulation strategies, parameter identification, artificial intelligence, operation under harsh or failure conditions, and modelling of electric or magnetic quantities in electric machines. Several chapters give an insight into the problem of minimizing losses in electric machines and increasing the overall energy efficiency of electric drives.

INTECH
open science | open minds

InTech Europe
University Campus STeP Ri
Slavka Krautzeka 83/A
51000 Rijeka, Croatia
Phone: +385 (51) 770 447
Fax: +385 (51) 686 166
www.intechopen.com

InTech China
Unit 405, Office Block, Hotel Equatorial Shanghai
No.65, Yan An Road (West), Shanghai, 200040, China
中国上海市延安西路65号上海国际贵都大饭店办公楼405单元
Phone: +86-21-62489820
Fax: +86-21-62489821

IntechOpen